DIAGNOSTICS OF RF BREAKDOWNS IN HIGH-GRADIENT ACCELERATING STRUCTURES

A. Palaia*, Uppsala University, Sweden

V. Dolgashev, J. Lewandowski, S. Weathersby, SLAC National Accelerator Laboratory, CA, USA

Abstract

Within the framework of the research on high-gradient accelerating structures for future linear colliders, diagnostics of radio-frequency (RF) breakdowns is of great importance to support the understanding of the vacuum breakdown process. Measurements of RF and electron and ion currents emitted during and after a breakdown can be used to calculate the properties of any objects responsible for such power reflection and charge emission. Possible breakdown models, breakdown localization and a time-scale of the process are here discussed and compared to dedicated measurements. First results are presented.

INTRODUCTION

The research on high-gradient accelerating structures is a key aspect for the development of TeV-scale linear lepton colliders. The Compact Linear Collider (CLIC) is one of these projects, an electron-positron collider relying on a two-beam acceleration scheme based on 12 GHz room temperature accelerating structures to accelerate beams up to 3 TeV. The demand to reach such energies within a reasonable length requires an accelerating gradient of 100 MV/m. One of the key issues of structures providing such gradient is represented by vacuum breakdowns. Such processes would perturb the beam during normal machine operations, therefore their rate must be kept low. High power test facilities and dedicated measurements are therefore needed to achieve a proper structure conditioning and to better understand breakdowns' microscopic dynamics.

We report here about breakdown experiments carried on at the Accelerator Structure Test Area (ASTA) at SLAC, with a T18 travelling wave structure [1] under test in a resonant ring [2] (its main parameters are summarized in Table 1). Although the microscopic development of breakdowns is not well understood, a strong field reflection and charge emission during such processes can be clearly measured. We built diagnostics at ASTA to measure such signals and we present here our first attempt to analyse the data.

THE RESONANT RING AT ASTA

A schematic of the resonant ring at ASTA is shown in Fig. 1. It allows high power structure testing in a two-arm wave guide loop meant to recirculate the field such that it constructively interferes with itself increasing the power level in the structure at every turn. It is fed with a 11.4 GHz

* andrea.palaia@physics.uu.se

Table 1: Main Parameters of the T18 Structure

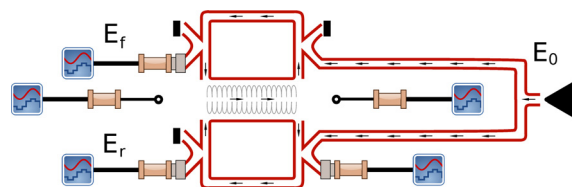|	
Frequency	11.424 GHz
Cells	18 + input cell + output cell
Filling time	36 ns
a_{in} / a_{out}	4.06/2.66 mm
$v_{g(input)}$ / $v_{g(output)}$	2.61/1.02 % of c
Phase advance/cell	120°
Unloaded gradient	55.5 MW → 100 MV/m

Figure 1: Sketch of the experimental set-up (not to scale).

field E_0, measured in a Peak Power Meter (PPM) with a sampling time of 10 ns (on the right of Fig 1). It is a 200 ns long pulse providing 70 MW in the first half and half such power in the second half. Such field is picked up by a directional coupler and measured before being split and sent to the two ring-arms through hybrids. It is then measured again by the upper directional coupler in one of the two arms on the left of Fig. 1, before it enters the structure. We refer to it as the forward field E_f. The lower arm is also equipped with a directional coupler which is used to measure any field E_r reflected from the structure in case of breakdowns. The forward and reflected field measurement points can be considered symmetric and at the same distance from the structure. The field picked up by directional couplers is down-mixed with a local oscillator signal to 200 MHz and sampled at a rate of 2 Gs/s. A typical breakdown event is shown in Fig. 2.

For the sake of simplicity the whole system can be thought of two parts: the first going from where E_0 is measured to where E_f is measured; the second part consisting of a complete ring-arm round trip, including wave guides and the accelerating structure. The travelling time t_1 of the first part is about 14 ns and the round trip time t_2 is 48 ns. Field attenuation and phase shift can be expressed in each one of these two sections by the complex numbers $c_1 = e^{i(\phi+i\alpha)}$ and $c_2 = e^{i(\psi+i\eta)}$, where α and η define ohmic losses and ϕ and ψ define phase shifts. The field E_f measured at time t is

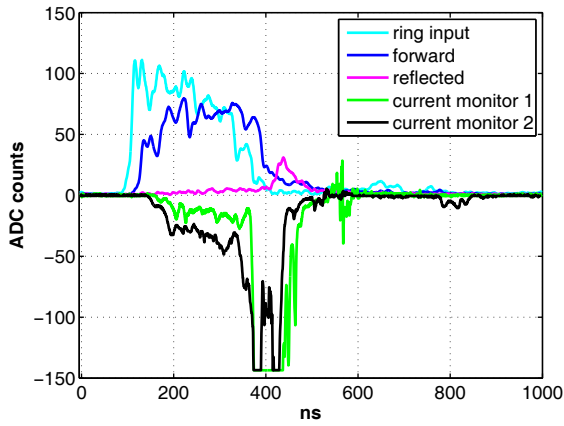$$E_f(t) = c_1 E_0(t-t_1) + c_2 E_f(t-t_2) \qquad (1)$$

Figure 2: Typical RF (field envelope) and current measurements from a breakdown event.

The latter is an over-determined system of t equations in the unknown c_1 and c_2 which can be solved by a pseudo-inverse in the following way:

$$\begin{pmatrix} c_1 \\ c_2 \end{pmatrix} = \beta = (A^T A)^{-1} A^T \mathbf{E_f} \qquad (2)$$

where

$$\mathbf{E_f} = \begin{pmatrix} E_f(0) \\ \vdots \\ E_f(t) \end{pmatrix}, A = \begin{pmatrix} E_0(-t_1) & E_f(-t_2) \\ \vdots & \vdots \\ E_0(t-t_1) & E_f(t-t_2) \end{pmatrix} \qquad (3)$$

The errors $\Delta\beta_i$ on the coefficients are

$$\Delta\beta_i^2 = \sigma^2 (A^T A)_{ii}^{-1} = \sigma^2 C_{ii} \qquad (4)$$

where C_{ii} is the covariance matrix and σ is the error on the field measurement.

RF BREAKDOWN LOCALIZATION

A breakdown in the structure causes the field to be reflected backwards. The reflected field keeps therefore the memory of the breakdown location as the difference of its phase with the phase of the forward field. Given the complex fields $E_f(t) = E_f e^{i[\omega t + \phi]}$ and $E_r(t) = E_r e^{i[\omega t + \psi]}$ - numerically derived from the real measured signals by means of a Hilbert transform - we down-mix them with another signal of angular frequency $\omega + \Delta\omega$ ($\Delta\omega \ll \omega$) and phase θ to obtain the slow-varying signals

$$\tilde{E}_f(t) = E_f e^{-i[\Delta\omega t - (\phi - \theta)]} \qquad (5)$$

$$\tilde{E}_r(t) = E_r e^{-i[\Delta\omega t - (\psi - \theta)]} \qquad (6)$$

where we remove the fast oscillating field at the sum frequency by passing the mixing product through a single pole IIR filter with a cutoff frequency of 500 MHz. Their instantaneous phases are

$$\chi(t) = \arg\left[\tilde{E}_f(t)\right] = \Delta\omega t - (\phi - \theta) \qquad (7)$$

$$\xi(t) = \arg\left[\tilde{E}_r(t)\right] = \Delta\omega t - (\psi - \theta) \qquad (8)$$

Hence the phase difference δ between forward and reflected field is

$$\delta = \chi(t) - \xi(t) = \arg\left(\frac{\tilde{f}}{\tilde{r}}\right) = \phi - \psi \qquad (9)$$

The phase difference distribution of a sample of 107 breakdown events is shown in Fig. 3. All events accumulate in three distinct populations separated by a distance of about $120°$, suggesting that breakdowns are localized on the irises of each cell of the $2\pi/3$ structure.
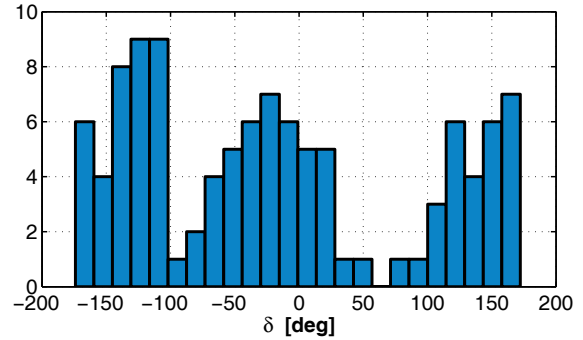

Figure 3: Phase difference between forward and reflected field in presence of breakdowns. The three distinct populations separated by about $120°$ suggest that breakdowns happen on the irises of each cell.

To calculate uniquely the location of each breakdown in the structure we use the time information given by the instant t_{r10} at which the reflected field appears (calculated at 10% of the maximum) and the instant t_{f90} at which the forward field shows missing power (calculated at 90% of the maximum). The time t_b from when the field is reflected until it is measured is

$$t_b = \frac{1}{2}\left(t_{r10} - t_{f90} + t_2\right) \qquad (10)$$

The distribution of breakdowns along the structure is shown in Fig. 4. The combined time and phase information from 107 breakdown events are summarised in Fig. 5,
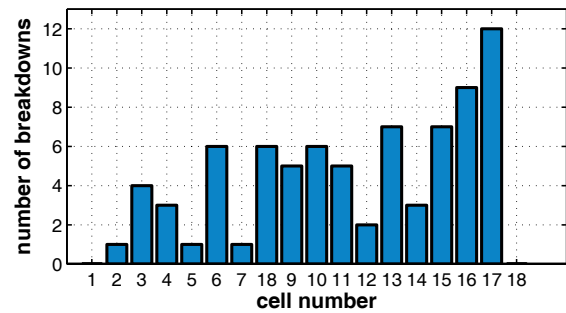

Figure 4: Distribution of breakdowns along the structure: number of breakdowns per cell.

where each blue dot represents a breakdown and the red crosses represent each cell together with the correspondent filling time in the $2\pi/3$ structure.
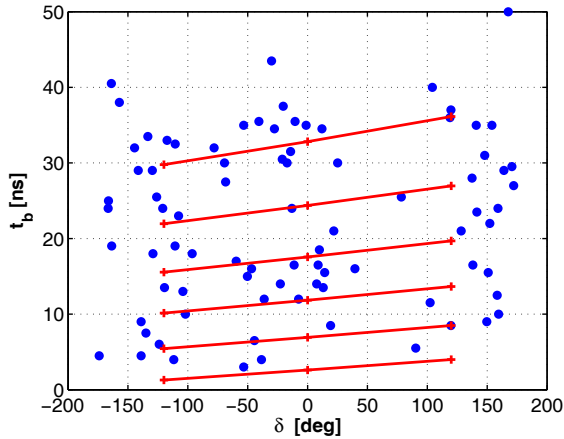

Figure 5: Calculated breakdown position (blue dots) with respect to the position of the irises in the structure (red crosses).

CHARACTERIZATION OF RF BREAKDOWNS

When a breakdown happens the field E_f propagates in the structure for a distance l until it is (partially) reflected backwards. A time t_b after it is reflected we measure

$$E_r(t) = \tilde{\Gamma} E_f(t - t_b) \qquad (11)$$

where $\tilde{\Gamma} = e^\gamma \Gamma$ is a complex factor taking into account twice the attenuation γ of the field over the distance l, and the complex reflection coefficient Γ. The fraction of the field which is not reflected will still be recirculating in the ring but the missing field will show at time t as follows:

$$E_f(t) \quad = c_1 E_0(t - t_1) + c_2 E_f(t - t_2) + \\ - \frac{c_2}{e^\gamma} E_r(t - t_2 + 2t_b) \qquad (12)$$

The RF reflection from the breakdown can be thought as the reflection due to a mismatched load of normalized impedance z_L in a microwave circuit. We consider here Eq. 11 and the reflection coefficient $\tilde{\Gamma}$ which keeps the memory of the breakdown location and its dissipative effect plus the ohmic losses along the line, as we are not able to disentangle the two contributions. Assuming that the object responsible for the reflection is characterized by the complex permittivity ϵ_r and by a unitary magnetic permeability,

$$z_L = \sqrt{\epsilon_r} = \frac{1 - \tilde{\Gamma}}{1 + \tilde{\Gamma}} \qquad (13)$$

The last equation suggests that we can test different breakdown scenarios comparing their permittivity with the reflection coefficient $\tilde{\Gamma}$. We explore here the possibility

that the RF reflection is caused by a plasma grown in the structure during the breakdown. We also assume a non-collisional and quasi-neutral plasma. Its permittivity is

$$\epsilon_r(\omega) = 1 - \frac{\omega_p^2}{\omega^2}, \qquad \omega_p = \frac{Nq^2}{m\epsilon_0} \qquad (14)$$

where ω_p is the plasma frequency, N is the charge density per cubic centimetre, e is the electric charge, m is the mass of the charged particles (electrons), ω the frequency of the incident wave and ϵ_0 the vacuum electric permittivity. The estimated peak value of the charge density N for a sample of 107 breakdown events is shown is Fig. 6. The average density of charges $N = 5 \cdot 10^{15}$ electrons per cubic centimetre is in agreement with the one estimated in previous experiments [3].
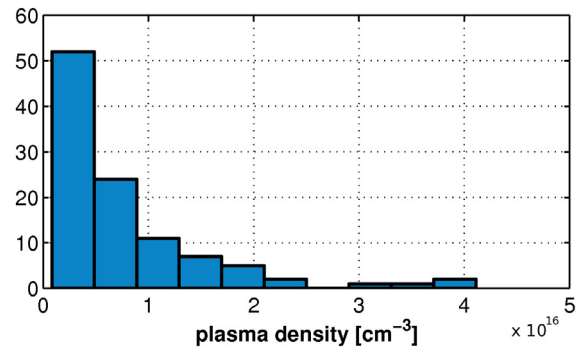

Figure 6: Distribution of the estimated plasma density which would cause the measured RF reflection.

ACKNOWLEDGEMENTS

REFERENCES

[1] R. Zennaro et al., "Design and Fabrication of CLIC Test Structures", Proceedings of the XXIV Linear Accelerator Conference, Victoria (British Columbia) 2008

[2] S. Tantawi, "Research and Development for Ultra High Gradient Accelerator Structures ", Talk at the Advanced Accelerator Concept Workshop, Annapolis 2010, http://www.ireap.umd.edu/AAC2010/tantawi.pdf

[3] M. Johnson et al., "Arrival time measurements of ions accompanying RF breakdown", Nuclear Instruments and Methods in Physics Research Section A, 595, 568 571 (2008), DOI:10.1016/j.nima.2008.08.001.